Resolution of subwavelength transmission devices formed by a wire medium

Pavel A. Belov
Department of Electronic Engineering, Queen Mary University of London, Mile End Road, London, E1 4NS, United Kingdom and Photonics and Optoinformatics Department, St. Petersburg State University of Information Technologies, Mechanics and Optics, Sablinskaya 14, 197101, St. Petersburg, Russia

Mario G. Silveirinha
Departamento de Engenharia Electrotécnica da Universidade de Coimbra, Instituto de Telecomunicações, Pólo II, 3030 Coimbra, Portugal

(Received 15 November 2005; revised manuscript received 21 March 2006; published 18 May 2006)

The restrictions on the resolution of transmission devices formed by wire media (arrays of conductive cylinders) recently proposed in Phys. Rev. B **71**, 193105 (2005) and experimentally tested in Phys. Rev. B **73**, 033108 (2006) are studied in this paper using both analytical and numerical modeling. It is demonstrated that such transmission devices have subwavelength resolution that can in principle be made as fine as required by a specific application by controlling the lattice constant of the wire medium. This confirms that slabs of the wire medium are unique imaging devices at the microwave frequency range, and are capable of transmitting distributions of TM-polarized electric fields with nearly unlimited subwavelength resolution to practically arbitrary distances.

DOI: 10.1103/PhysRevE.73.056607 PACS number(s): 42.70.Qs, 78.20.Ci, 42.25.Fx, 73.20.Mf

I. INTRODUCTION

The resolution of common imaging systems is restricted by the so-called diffraction limit, since these systems operate only with propagating spatial harmonics emitted by the source. The conventional lenses cannot transport evanescent harmonics which carry subwavelength information, since these waves exhibit exponential decay in natural materials and even in free space. Recently, a new type of device capable of transmitting images with subwavelength resolution was suggested in [1]. These structures are formed by planar slabs of materials with specific electromagnetic properties which make it possible to transfer images from one interface to another with subwavelength resolution. Such regime of operation is called canalization. This regime dramatically differs from the subwavelength imaging principle formulated in [2] which employs effects of negative refraction and amplification of evanescent waves. The idea is that both propagating and evanescent harmonics of a source can be transformed into the propagating waves inside of a slab of an electromagnetic crystal. Then, these propagating modes can transmit subwavelength images from one interface of the slab to the other one.

In order to implement the canalization regime it is required to use materials in which the electromagnetic waves have a flat isofrequency contour. Such media are capable of transmitting energy only in one direction, always with the same phase velocity. The typical example of such materials is the wire medium (see Fig. 1), which consists of an array of parallel, ideally conducting wires [3–6], operating at frequencies smaller than its characteristic plasma frequency. The wire medium supports transmission line modes which travel along the wires at the speed of light. A slab of wire medium with thickness equal to an integer number of half-wavelengths experiences Fabry-Perot resonance for any angle of incidence, including complex ones, and thus such a slab is capable of transporting images with subwavelength resolution [7]. The transmission devices formed by wire medium were studied both numerically and experimentally in [7]. As a result, the imaging with $\lambda/15$ resolution has been successfully demonstrated. In [7] it was assumed that the structure operates at a very low frequency as compared to its plasma frequency, and no estimation has been made on how the plasmalike properties of the wire medium could affect the operation of such devices. In order to reveal the restrictions on the resolution caused by plasmalike properties of the wire medium, in the present paper we theoretically study the transmission through a wire medium slab using the additional boundary condition recently formulated in [8]. The wire medium is modeled as a homogeneous material described by an effective permittivity tensor. The theoretical

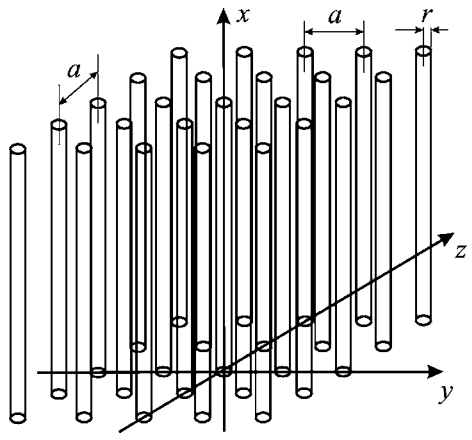

FIG. 1. The geometry of the wire medium: A square lattice of parallel, ideally conducting thin wires.

results are validated using the full wave periodic method of moments [9], which models every detail of the structure and the actual granularity of the material. It is proved that the effective material model is sufficiently accurate to model the electromagnetic response of the wire medium.

The paper is organized as follows. After a brief introduction, the expressions of the reflection and transmission coefficients for a planar slab of wire medium are presented. In the third section, the transmission and reflection properties are studied for various frequencies of operation using both theoretical and numerical modeling. The fourth section is devoted to the study of resolution using the Rayleigh criterion. The imaging accuracy and the theoretical limit of resolution are studied in the fifth section using a half-intensity criterion. Finally, the conclusion is presented. Also, the paper is accompanied by an appendix where guided modes in slabs of wire medium are investigated.

II. REFLECTION AND TRANSMISSION COEFFICIENTS FOR A WIRE MEDIUM SLAB

The wire medium is a material characterized by strong spatial dispersion even at low frequencies [6]. It can be described by a spatially dispersive permittivity tensor of the form

$$\bar{\bar{\varepsilon}} = \varepsilon \mathbf{xx} + \mathbf{yy} + \mathbf{zz}, \quad \varepsilon(\omega, q_x) = 1 - \frac{k_p^2}{k^2 - q_x^2}, \tag{1}$$

where the x axis is oriented along wires, q_x is the x component of wave vector $\mathbf{q}$, $k=\omega/c$ is the wave number of the host medium, c is the speed of light, and $k_p=\omega_p/c$ is the wave number corresponding to the plasma frequency ω_p. The plasma frequency depends on the lattice period a and on the radius of wires r [10],

$$k_p^2 = \frac{2\pi/a^2}{\ln \dfrac{a}{2\pi r} + 0.5275}. \tag{2}$$

Note that in this paper we assume that the metallic wires are arranged in a square lattice. The permittivity tensor is normalized to the permittivity of the host medium.

The solution of any boundary problem involving the wire medium (using an effective medium theory) requires the knowledge of an additional boundary condition at the interface. In fact, it has long been known that the usual boundary conditions (continuity of the tangential components of the electromagnetic field) are insufficient in case of spatial dispersion [11–13]. Such an additional boundary condition has been formulated in [8] for the wire medium case. It was proved that the normal component of the electric field must be continuous at the interface between the wire medium and free space, under the condition that the host medium of the wire medium is also free space. In this paper, we will use this result to study the resolution of the transmission devices formed by the wire medium. First, we characterize the scattering of plane waves by a wire medium slab.

Let us consider a slab of wire medium with thickness d (see Fig. 2). We suppose that the wires stand in free space and are normal to the interface. The wires are assumed perfectly conducting, i.e., losses are assumed negligible. The distribution of the electromagnetic field at the input plane of the transmission device can be decomposed in terms of spatial harmonics. The spatial harmonics are either propagating plane waves or evanescent plane waves, and their polarization can be classified as transverse electric (TE) or transverse magnetic (TM) with respect to the orientation of the wires. In [7] it was proved that a slab of the wire medium allows subwavelength imaging of the part of the spatial spectrum with TM polarization.

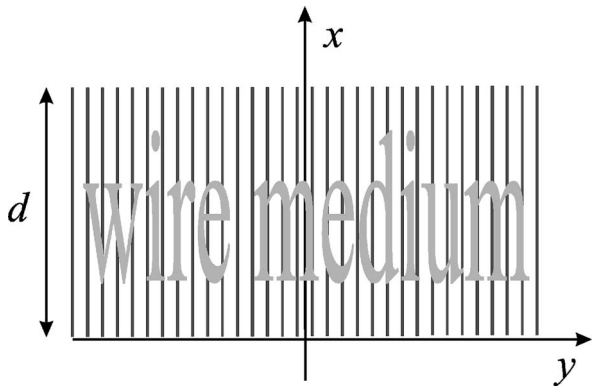

FIG. 2. The wire medium slab. The structure is unbounded and periodic along the y- and z directions.

To determine the resolution of the imaging, we consider that a plane wave with TM polarization impinges on the slab. Let H_{inc} be the amplitude of the incident magnetic field along the z direction, and let $\mathbf{k}=(k_x,k_y,0)^T$ be the wave vector of the incident wave. The x component of the wave vector k_x can be expressed in terms of the wave number k and of the y component of the wave vector k_y as $k_x=-j\sqrt{k_y^2-k^2}$. The incident plane wave excites two types of waves in the wire medium: the extraordinary wave (TM mode) and the transmission line (TEM) mode [6]. The ordinary wave is not excited since it has TE polarization. The tangential component of the wave vector k_y is preserved at the interface between free space and the wire medium. Using this property we can evaluate the wave vector associated with each of the excited modes in the slab. The wave vector associated with transmission line modes is of the form

$$\mathbf{q}_{\pm}^{\text{TEM}} = (\pm k, k_y, 0)^T. \tag{3}$$

These waves travel along the wires with the speed of light in free space, independently of the value of transverse component of wave vector k_y. On the other hand, the extraordinary modes obey the dispersion equation derived in [6],

$$q_x^2 + q_y^2 + q_z^2 = k^2 - k_p^2, \tag{4}$$

and thus the wave vector of an extraordinary mode is of the form

$$\mathbf{q}_{\pm}^{\text{TM}} = (\pm q_x, k_y, 0), \quad q_x = -j\sqrt{k_p^2 + k_y^2 - k^2}. \tag{5}$$

If the frequency of operation is smaller then the plasma frequency ($k<k_p$), then the extraordinary modes are evanes-

cent: the x component of wave vector q_x is a purely imaginary number for any real k_y. In order to emphasize this fact it is convenient to use the notation $q_x=-j\gamma_{\mathrm{TM}}$, with $\gamma_{\mathrm{TM}}=\sqrt{k_p^2+k_y^2-k^2}$. Also, by analogy, we denote $k_x=-j\gamma_x$ with $\gamma_x=\sqrt{k_y^2-k^2}$. The value of γ_x is purely imaginary if $k_y<k$ (propagating modes in free space), but it becomes a real number if $k_y>k$ (evanescent modes in free space, i.e., the subwavelength spatial spectrum).

The total magnetic field (directed along the z axis) can be written in the following form:

$$\frac{H(x)}{H_{\mathrm{inc}}}=\begin{cases}e^{-jk_xx}+Re^{jk_xx}, & x<0\\ A_-^{\mathrm{TM}}e^{-\gamma_{\mathrm{TM}}(x-d/2)}+A_+^{\mathrm{TM}}e^{+\gamma_{\mathrm{TM}}(x-d/2)}+A_-^{\mathrm{TEM}}e^{-jk(x-d/2)}+A_+^{\mathrm{TEM}}e^{+jk(x-d/2)}, & 0\leqslant x\leqslant d\\ Te^{-jk_x(x-d)}, & x>d,\end{cases} \tag{6}$$

where R and T are the reflection and transmission coefficients, $A_\pm^{\mathrm{TM}}$ and $A_\pm^{\mathrm{TEM}}$ are the amplitudes of the extraordinary (TM) and transmission line (TEM) modes in the slab, respectively.

Following [8], all components of both magnetic and electric fields are continuous at the interface between free space and the wire medium. Thus, the magnetic field $H(x)$ and both its first $dH(x)/dx$ and second $d^2H(x)/dx^2$ derivatives by x are continuous at interfaces $x=0$ and $x=d$. This can be written using (6) in the form of the following system of equations:

$$\begin{pmatrix}-1 & e^{\gamma_{\mathrm{TM}}d/2} & e^{-\gamma_{\mathrm{TM}}d/2} & e^{jkd/2} & e^{-jkd/2} & 0\\ -jk_x & -\gamma_{\mathrm{TM}}e^{\gamma_{\mathrm{TM}}d/2} & \gamma_{\mathrm{TM}}e^{-\gamma_{\mathrm{TM}}d/2} & -jke^{jkd/2} & jke^{-jkd/2} & 0\\ k_x^2 & \gamma_{\mathrm{TM}}^2e^{\gamma_{\mathrm{TM}}d/2} & \gamma_{\mathrm{TM}}^2e^{-\gamma_{\mathrm{TM}}d/2} & -k^2e^{jkd/2} & -k^2e^{-jkd/2} & 0\\ 0 & e^{-\gamma_{\mathrm{TM}}d/2} & e^{\gamma_{\mathrm{TM}}d/2} & e^{-jkd/2} & e^{jkd/2} & -1\\ 0 & -\gamma_{\mathrm{TM}}e^{-\gamma_{\mathrm{TM}}d/2} & \gamma_{\mathrm{TM}}e^{\gamma_{\mathrm{TM}}d/2} & -jke^{-jkd/2} & jke^{jkd/2} & jk_x\\ 0 & \gamma_{\mathrm{TM}}^2e^{-\gamma_{\mathrm{TM}}d/2} & \gamma_{\mathrm{TM}}^2e^{\gamma_{\mathrm{TM}}d/2} & -k^2e^{-jkd/2} & -k^2e^{jkd/2} & k_x^2\end{pmatrix}\begin{pmatrix}R\\ A_-^{\mathrm{TM}}\\ A_+^{\mathrm{TM}}\\ A_-^{\mathrm{TEM}}\\ A_+^{\mathrm{TEM}}\\ T\end{pmatrix}=\begin{pmatrix}1\\ -jk_x\\ -k_x^2\\ 0\\ 0\\ 0\end{pmatrix}. \tag{7}$$

Solving this system, the reflection and transmission coefficients can be expressed as follows:

$$R=1-\frac{1}{1+\frac{\gamma_{\mathrm{TM}}k_y^2}{\gamma_x(k_y^2+k_p^2)}\tanh\left(\frac{\gamma_{\mathrm{TM}}d}{2}\right)-\frac{kk_p^2}{\gamma_x(k_y^2+k_p^2)}\tan\left(\frac{kd}{2}\right)}-\frac{1}{1+\frac{\gamma_{\mathrm{TM}}k_y^2}{\gamma_x(k_y^2+k_p^2)}\mathrm{ctanh}\left(\frac{\gamma_{\mathrm{TM}}d}{2}\right)+\frac{kk_p^2}{\gamma_x(k_y^2+k_p^2)}\mathrm{ctan}\left(\frac{kd}{2}\right)}, \tag{8}$$

$$T=\frac{1}{1+\frac{\gamma_{\mathrm{TM}}k_y^2}{\gamma_x(k_y^2+k_p^2)}\tanh\left(\frac{\gamma_{\mathrm{TM}}d}{2}\right)-\frac{kk_p^2}{\gamma_x(k_y^2+k_p^2)}\tan\left(\frac{kd}{2}\right)}-\frac{1}{1+\frac{\gamma_{\mathrm{TM}}k_y^2}{\gamma_x(k_y^2+k_p^2)}\mathrm{ctanh}\left(\frac{\gamma_{\mathrm{TM}}d}{2}\right)+\frac{kk_p^2}{\gamma_x(k_y^2+k_p^2)}\mathrm{ctan}\left(\frac{kd}{2}\right)}. \tag{9}$$

In the above "tanh" and "ctanh" represent the hyperbolic tangent and cotangent, respectively. The canalization regime is observed for the slab under consideration when $kd=n\pi$, where n is an integer. In this case (9) can be simplified: if $kd=(2n+1)\pi$ then

$$T=-\frac{1}{1+\frac{\gamma_{\mathrm{TM}}k_y^2}{\gamma_x(k_y^2+k_p^2)}\mathrm{ctanh}(\gamma_{\mathrm{TM}}d/2)},\quad R=1+T, \tag{10}$$

whereas if $kd=2n\pi$ then

$$T=\frac{1}{1+\frac{\gamma_{\mathrm{TM}}k_y^2}{\gamma_x(k_y^2+k_p^2)}\tanh(\gamma_{\mathrm{TM}}d/2)},\quad R=1-T. \tag{11}$$

The transmission coefficient calculated above can be regarded as a transfer function: the image at the output plane is obtained by superimposing the (TM-polarized) spatial harmonics of the source field distribution at the input plane multiplied by T. Strictly speaking, that is not rigorously true, even if the exact expression for transmission coefficient is known. Indeed, when doing this we are neglecting the higher order harmonics, which decay much faster than the fundamental mode, but also contribute to the near field. These harmonics are a manifestation of the actual granularity of wire medium, and are not described by the effective medium model (1). The contribution of the high-order harmonics can be neglected while $k_ya<\pi$, which corresponds to operation below the ultimate limit of resolution $\Delta_l=a$ [14]. In this case, slight variations of the near field near the edges of the wires do not influence the resolution of the device. Thus, in this paper we will consider that the distribution of the field at the output plane is equal to the distribution of the field at the

input plane multiplied by the transmission coefficient. Within this approximation, it is sufficient to characterize T in order to evaluate the resolution of the transmission device.

If the operating frequency is much smaller than the plasma frequency, i.e., $k \ll k_p$, then since $kd/\pi > 1$ we can assume that $\gamma_{\mathrm{TM}} d \gg 1$, and using the expressions (10) and (11) we obtain simple approximate formulas for the reflection and transmission coefficients,

$$T \approx \mp \frac{1}{1 + \dfrac{\gamma_{\mathrm{TM}} k_y^2}{\gamma_x (k_y^2 + k_p^2)}}, \quad R \approx 1 - \frac{1}{1 + \dfrac{\gamma_{\mathrm{TM}} k_y^2}{\gamma_x (k_y^2 + k_p^2)}}, \tag{12}$$

where the $\mp$ sign corresponds to the case in which the thickness of the slab is equal to an even or odd number of half-wavelengths, respectively.

Some important properties of (10) and (11) are readily identified. It is clear that if $k_p \to \infty$ then $T \approx \mp 1$ for any k_y, and therefore, in such conditions the imaging is perfect for this polarization. On the other hand, one can see that $T=0$ when $\gamma_x = 0$, i.e., $k_y = k$. This property is very important because it shows that the spatial harmonics with $k_y = k$ are filtered by the WM, which some how contradicts the subwavelength imaging. Actually, as it will be demonstrated below, the band of the spatial harmonics corresponding to this filtering is so narrow that it practically does not affect the imaging properties of the system.

It is noteworthy that if $k_y \to \infty$ then $T \to \mp 1/2$ [21]. This means that the spatial harmonics in the deep subwavelength spectrum are transferred from the source to the image plane, but, in contrast to the spatial harmonics with smaller k_y, their amplitude will be reduced two times. Thus, the transfer function of the imaging device is not perfect since it is not a constant function of the transverse wave vector. Nevertheless, it will be shown that this fact does not significantly affect the subwavelength imaging performance of the device.

Also, it is clear that the imaging quality does not depend on the thickness of the structure. The transmission device can be made as thick as may be required by an application. The only restriction is that the thickness has to be equal to an integer number of half-wavelengths. If the number of half-wavelengths is odd, then the image at the back interface of the structure will appear out of phase with respect to the source, whereas if the number of half-wavelengths is even, then the image and the source will be in phase. Moreover, the bandwidth of operation does not depend on the thickness of the transmission device. It remains the same for all slab thicknesses equal to the integer number of half-wavelengths.

III. PARAMETRIC STUDY OF REFLECTION AND TRANSMISSION PROPERTIES

In [7] the wire medium with period $a=1$ cm formed by wires with $r=1$ mm has been considered. Substitution of these parameters into (2) gives $k_p a = 2.5$. A more accurate value, calculated using the numerical method proposed in [15], is $k_p a = 2.36$. The frequency of operation for the transmission device in [7] was 1 GHz, which corresponds to $ka = 0.2$, and the thickness $d=15$ cm of the structure was chosen equal to half-wavelength, that is $kd = \pi$, or in terms of the wave number corresponding to the plasma frequency $k_p d/\pi = 11.3$. In the present paper we consider the same parameters for the transmission device.

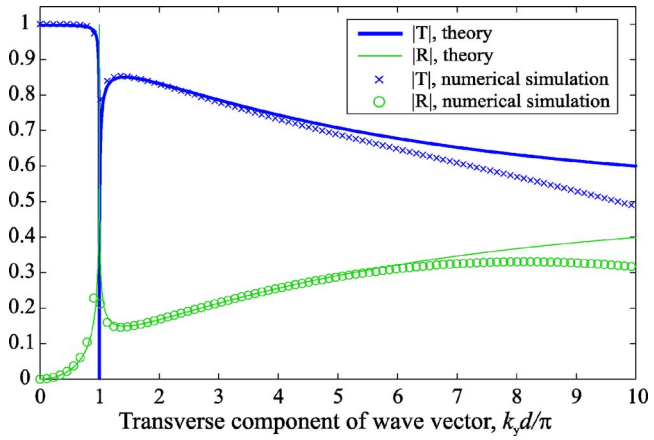

FIG. 3. (Color online) Reflection (R) and transmission (T) coefficients (absolute values) as a function of the transverse component of wave vector $k_y d/\pi$ for $kd/\pi = 1$. Solid lines: analytical expressions (8) and (9). Crosses and circles: points calculated using full wave numerical method.

The dependence of the reflection and transmission coefficients (absolute values) on the normalized transverse component of wave vector $k_y d/\pi$ is plotted in Fig. 3. One can see that the transmission coefficient has a very sharp dip at $k_y = k$, but for other values of k_y it has values close to unity. In Fig. 3 the "crosses" and "circles" represent the data calculated numerically using the periodic method of moments. As seen, the agreement between the analytical model and the full wave results is very satisfactory. We do not present a plot for the phase of transmission coefficient since it is practically equal to π for the whole range of k_y, except for a very narrow band with upper bound equal to k. The obtained dependence confirms that the slab indeed operates in the canalization regime and is capable of transporting subwavelength images with TM polarization.

The behavior of the transmission and reflection coefficients is sensitive to variations in the frequency of operation. In Fig. 4, the transmission characteristic is depicted for frequencies that are lower than original frequency of operation by 0.2%, 0.4%, 0.6%, and 0.8%. It is seen that the amplitude of the evanescent modes is amplified in a certain range of k_y.

The further decrease of the frequency of operation reveals a very interesting resonant phenomenon. This is illustrated in Fig. 5, where the transmission coefficient is plotted for frequencies which lower than the design frequency by 1%, 2%, 3%, 4%, and 6%. One can observe a very strong enhancement of certain spatial harmonics. This property reveals the presence of guided modes propagating along the y direction of the slab, the mechanism of propagation being closely related to that of an Yagi antenna array [16]. The dispersion properties of the guided modes are studied in the Appendix. The observed resonant enhancement deteriorates the subwavelength imaging since some of the spatial harmonics happen to be amplified by a factor of 10 or even more.

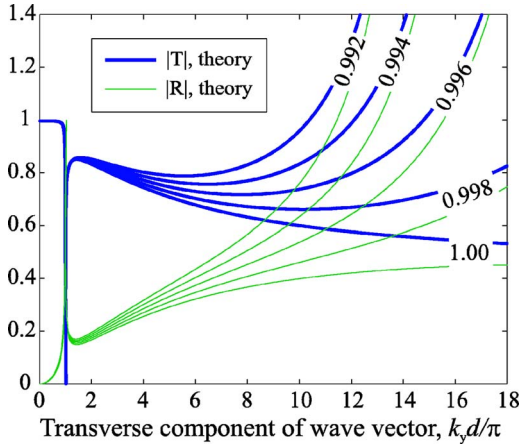

FIG. 4. (Color online) Reflection (R) and transmission (T) coefficients (absolute values) as a function of the transverse component of wave vector $k_y d/\pi$ for $kd/\pi=1-0.002n$, where $n=0,1,2,3,4$. The numbers in the figure correspond to the values of kd/π.

For frequencies slightly larger than the frequency corresponding to the Fabry-Perot resonance, the reflection and transmission coefficients do not have a resonant behavior. This is shown in Fig. 6, where the reflection and transmission coefficients are plotted for frequencies larger than the design frequency by 1%, 2%, and 4%. This means that the slab does not support guided modes in this frequency range. Further increase of the frequency (by 8% or 16%, for example, see Fig. 6) leads to the increase of the width of the narrow dip of the transmission characteristic at $k_y=k$, and to the appearance of resonances in the vicinity of this point. These resonances (shown with greater detail in Fig. 7) are also related to guided modes. The dispersion branch of these modes appears near the light line in Fig. 12. The resonant behavior in the present case has a very narrow-band character and does not significantly affect the imaging properties of the device.

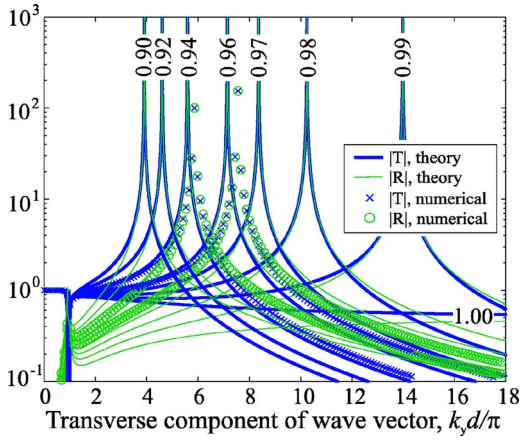

FIG. 5. (Color online) Reflection (R) and transmission (T) coefficients (absolute values) as a function of the transverse component of wave vector $k_y d/\pi$ for $kd/\pi=1-0.01n$, where $n=0,1,2,3,4,6$. The numbers in the figure correspond to the values of kd/π. The crosses and circles represent the results of the numerical modeling for $kd/\pi=0.94$ and $kd/\pi=0.96$.

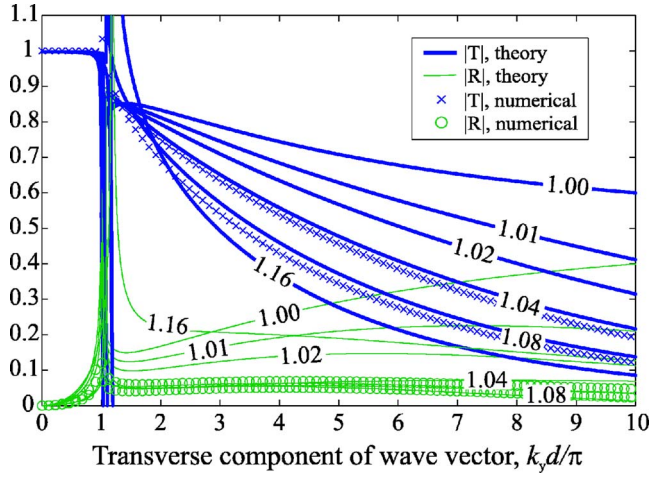

FIG. 6. (Color online) Reflection (R) and transmission (T) coefficients (absolute values) as a function of the transverse component of wave vector $k_y d/\pi$ for $kd/\pi=1+0.01n$, where $n=0,1,2,3,4,8,16$. The numbers in the figure correspond to the values of kd/π. The crosses and circles present the results of the numerical modeling for $kd/\pi=1.04$ and $kd/\pi=1.08$.

In Fig. 6 one can see a strong reduction of the reflection coefficient for $kd/\pi=1.04$ and $kd/\pi=1.08$. The reflection coefficient becomes less than 10% for practically the whole spatial spectrum. This fact has been numerically confirmed, and means that for these frequencies there is little interference between the source and the signal reflected at the wire medium slab.

IV. STUDY OF RESOLUTION

In order to study the resolution of the wire medium slab, we use the Rayleigh criterion: the resolution is taken equal to the radius of the image spot (at the half-intensity level) for a very sharp (nearly point) source. The resolution value obtained using this criterion corresponds to the half of the minimum distance between two sharp maxima that can be resolved using the imaging device.

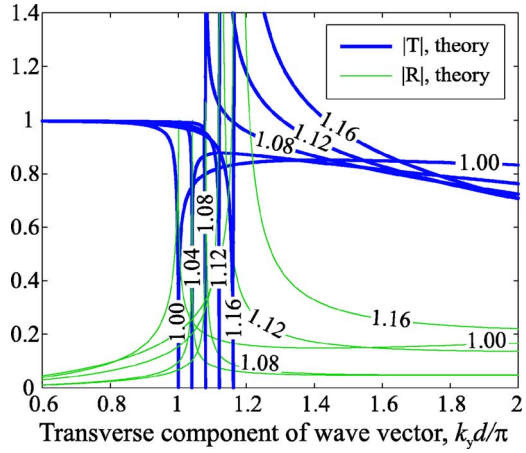

FIG. 7. (Color online) Reflection (R) and transmission (T) coefficients (absolute values) as a function of the transverse component of wave vector $k_y d/\pi$ for $kd/\pi=1+0.04n$, where $n=0,1,2,3,4$. The numbers in the figure correspond to the values of kd/π.

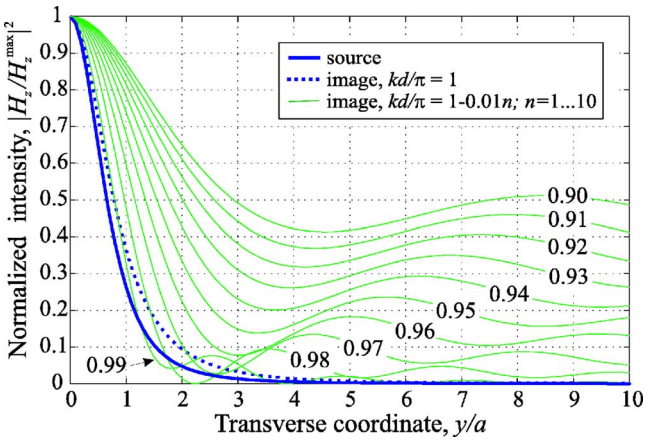

FIG. 8. (Color online) Image when the wire medium slab is illuminated with the source (14) at frequencies slightly smaller than $kd/\pi=1$. The numbers in the figure correspond to the values of the normalized frequency kd/π.

In order for the wire medium homogenization model to be used we are not allowed to consider any sources with radius much smaller than the real period of the structure. Indeed, the spatial spectrum of such a source contains important spatial harmonics in the range $k_y a \gg \pi$, whose propagation cannot be described by the homogenized model. Moreover, it was shown in [14] that the resolution of any periodic structure is limited by its period. Due to these reasons, below we consider a magnetic field distribution with diameter only slightly smaller than the period. The spectrum of the source at the front plane of the wire medium slab is

$$s(k_y) = e^{-\sqrt{k_y^2 - k^2}a/2}. \tag{13}$$

Note that the spectrum is independent of k_z, and consequently the field intensity is uniform along the z direction. This two-dimensional source has the magnetic field distribution

$$H_z(y) = A\int_{-\infty}^{+\infty} s(k_y)e^{-jk_y y}dk_y$$

$$= Aj\pi H_1^{(2)}(k\sqrt{(a/2)^2 + y^2})\frac{a/2}{\sqrt{(a/2)^2 + y^2}}, \tag{14}$$

where $H_1^{(2)}(x)$ is the Hankel function of the second kind, and A is a constant that defines the amplitude of the source. The intensity of the field normalized by its maximum value $H_z^{max}=H_z(0)$ is plotted in Fig. 8 (thick solid line).

The distribution of magnetic field under consideration appears at the half-period distance from a plane with point source of magnetic field which has uniform spatial spectrum. Thus, expression (13) also represents the transmission coefficient for a slab of free space with the half-period thickness. This slab allows one to transform a singular distribution of the point source into less sharp distribution which is appropriate for our studies using effective medium theory. Note that the point source of magnetic field we are dealing with has nothing to do with magnetic line source (line of magnetic current flowing along the z direction)! The point source of magnetic field is a delta function of magnetic field in the plane $x=-a/2$ $[H_z(y)|_{x=-a/2}=\delta(y)]$, which means that the field in that plane is zero everywhere except at one singular point. We have chosen this source because of the simplicity of its exponentially decaying spatial spectrum (13) and since its field decays faster than the field created by a point magnetic source: the field of our source (14) decays inversely proportional to y, but the field radiated by a magnetic line source would decay as the inverse square root of y.

The magnetic field at the output plane when the slab is illuminated by the source is given by

$$H_z(y) = A\int_{-\infty}^{+\infty} s(k_y)T(k_y)e^{-jk_y y}dk_y. \tag{15}$$

The integral in (15) is singular and nonintegrable if the slab supports guided modes: some poles of the transmission coefficient (9) as a function of k_y are located at the real line (see the Appendix). These difficulties can be avoided if negligibly small losses are introduced into the permittivity of the host medium. The presence of losses shifts the poles away from the real line. This makes the integral nonsingular and it can be evaluated relatively easily using direct numerical integration. The integral (15) has been calculated for all values of kd/π considered in the previous section. The corresponding images at the output plane are plotted in Figs. 8 and 9 for frequencies below and above the first Fabry-Perot resonance, respectively. For $ka<0.93$ and $ka>1.5$ the image is distorted by the resonant guided modes of the slab with short and long wavelengths, respectively. On the other hand, for $0.93<ka/\pi<1.5$ the images have the same shape as the source and their radii vary from a to $2a$. This means that at these frequencies the resolution of the imaging device Δ is from $\lambda/30$ to $\lambda/15$. Note that $\Delta_l=\lambda/30=a$ is the ultimate limit of resolution imposed by the periodicity of the structure [14]. The resolution of $\lambda/15$ for the structure under consideration has been observed in [7] both numerically and experimentally. This allows us to conclude that the theoretical study presented in this paper is consistent with results re-

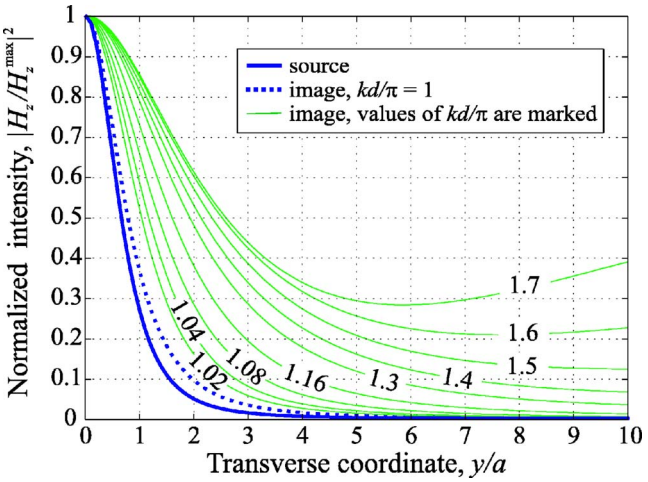

FIG. 9. (Color online) Image when the wire medium slab is illuminated with the source (14) at frequencies slightly larger than $kd/\pi=1$. The numbers in the figure correspond to the values of the normalized frequency kd/π.

ported in [7]. However, the presented analysis gives a much more comprehensive explanation of the limitations and characteristics of our imaging device.

V. ACCURACY OF IMAGING

The Rayleigh criterion used in the previous section is classical for imaging above the diffraction limit. However, near-field subwavelength imaging significantly differs from conventional imaging. Indeed, the latter requires that the source is placed very close to the interface of the imaging device. Hence, not only the transmission properties of the structure affect its performance, but also the reflection properties. If the reflection coefficient has large amplitude then the reflected field can interact with the source and modify its near-field pattern. This modified pattern will be transmitted with subwavelength resolution from the input plane to the output plane, but then it has nothing to do with the original source. As discussed in the previous section and seen in Figs. 4–6 the strong reflections from the slab of wire medium are mainly caused by the resonances associated with the guided modes. That is why the imaging with minimum reflections happens at the frequencies corresponding to the band gaps for the guided modes and slightly higher frequencies. Figure 6 clearly illustrates this statement: for $1.01 < kd/\pi < 1.16$ the reflection coefficient from the slab is smaller than 20%, and for $1.04 < kd/\pi < 1.08$ it is smaller than 10%.

Another important point concerning accuracy of the subwavelength imaging using slabs of wire media is that the transmission coefficient is different for different transverse components of the wave vector. As already mentioned, even if the thickness of the slab is tuned to fulfill Fabry-Perot condition (as in Fig. 3) the transmission coefficient is close to unity only in a limited range of spatial harmonics. For spatial harmonics with large k_y the transmission coefficient approaches $1/2$. This fact causes distortion in the image. It is possible to estimate the resolution at which the imaging device works with acceptable distortion. With this purpose we use the a half-intensity criterion: we assume that imaging with acceptable distortion happens while the transmission coefficient of spatial harmonics is in the range $[1/\sqrt{2}, \sqrt{2}]$. If

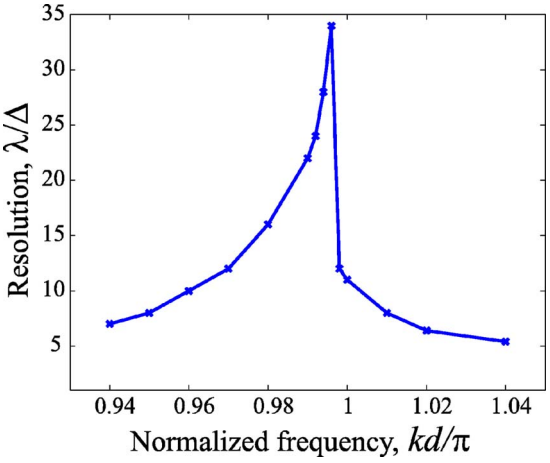

FIG. 10. (Color online) Normalized resolution λ/Δ as a function of the normalized frequency of operation kd/π.

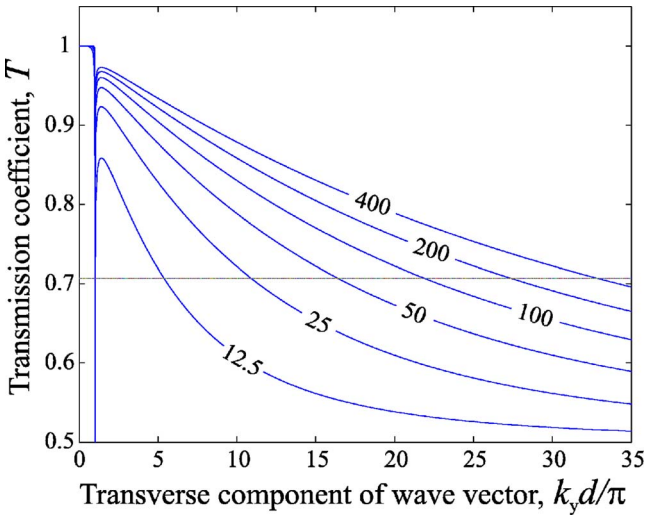

FIG. 11. (Color online) Dependence of the transmission coefficient T (absolute value) on transverse component of wave vector $k_y d/\pi$ for the case when $kd/\pi=1$ and various values of plasma frequency $k_p d/\pi = 12.5 \cdot 2^n$, where $n=0,1,2,3,4$. The numbers in the figure correspond to the values of $k_p d/\pi$

$k_y^{\max}$ is the maximum transverse wave vector component for which the half-intensity criterion is fulfilled then the resolution is $\Delta = \pi/k_y^{\max}$. This definition of resolution is stronger than the Rayleigh criterion. It guarantees not only that maxima at distance Δ are resolved, but also that the image is restored with little distortion.

For the case presented in Fig. 3, the transmission coefficient T is less than 1 and greater than $1/\sqrt{2}$ for $k_y d/\pi < 5$ except for the very narrow range of $k_y d/\pi$ close to 1. This means that the resolution of the transmission device under study is equal to $\Delta = \pi/k_y^{\max} = \lambda/10$. This value is only three times larger than the ultimate limit of resolution due to periodicity of the structure $\Delta_l = a = \lambda/30$ formulated in [14], and a bit worse than the real resolution of $2a = \lambda/15$ observed in [7].

A slight change of frequency may help improve the resolution of the device. For example, in the case of $kd/\pi = 0.996$ (see Fig. 4) the resolution happens to be equal to $\lambda/34$, which is even smaller than the ultimate limit dictated by periodicity. When $kd/\pi = 0.96$ the resolution is reduced to $\lambda/10$. One can verify that imaging with a resolution better than $\lambda/10$ is observed for $kd/\pi \in [0.96, 1.00]$. This means that the bandwidth of operation with $\lambda/10$ or better resolution is equal to 4% for the transmission device under consideration. The bandwidth of imaging with worse but still subwavelength resolution can be even larger. In [7] the 15% bandwidth of imaging with subwavelength resolution has been reported. We summarize our results for the dependence of the resolution (defined using the half-intensity criterion) on the frequency in Fig. 10. By tuning the frequency one can dramatically enhance the resolution. In practice this means that it is always possible to reach an ultimate limiting resolution $\Delta_l = a$ [14] by appropriately choosing the frequency of operation. The value of the resolution for the case $kd/\pi = 1$ approximately describes an average level of resolution of the system. This value can be evaluated analytically as explained next.

From Eq. (12) it is clear that for $k_y \gg k$ (subwavelength spatial spectrum) then

$$T \approx \mp \frac{1}{1+\frac{k_y}{\sqrt{k_y^2+k_p^2}}}. \quad (16)$$

Solving the equation $T(k_y^{\max})=1/\sqrt{2}$, we obtain

$$k_y^{\max} = \sqrt{\frac{\sqrt{2}-1}{2}}k_p \approx 0.455k_p. \quad (17)$$

Thus, the resolution $\Delta=\pi/k_y^{\max}$ for $kd/\pi=1$ is given by

$$\Delta = \frac{\pi}{0.455k_p} = 1.1\lambda\frac{k}{k_p} = 2.75a\sqrt{\ln\frac{a}{2\pi r}+0.5275}. \quad (18)$$

Thus, the smaller the ratio k/k_p is, the better is the resolution of the system. Formula (18) shows that the resolution of the wire medium slab is only limited by the ability to fabricate very dense arrays of wires, i.e., the limit of resolution only depends ultimately on the value of the lattice constant of the crystal. By decreasing the period of wire medium one can greatly improve resolution of the system. This fact is illustrated in Fig. 11, which shows the transmission characteristic calculated for different values of the plasma frequency. For extremely thin wires and very high frequencies the effect of losses may not be negligible. Nevertheless, at the microwave domain, this effect is expected to be of second order.

VI. CONCLUSION

In this paper, the resolution of subwavelength transmission devices formed by the slabs of wire media was studied. It was shown that the resolution does not depend on the thickness of the structure, which can in principle be made as thick as required by an application. By slightly tuning the frequency of operation, it is possible to achieve the ultimate limit on resolution dictated by the periodicity of the system (lattice constant of the crystal), even though this regime is narrow band. The average level of resolution ultimately depends on the period of the lattice. By reducing the lattice constant it may be possible to realize imaging systems with virtually no limit of resolution. This makes the slab of the wire medium a unique imaging device capable of transmitting a distribution of TM-polarized electric field with subwavelength resolution at the microwave frequency range.

ACKNOWLEDGMENT

The authors would like to thank Professor Constantin Simovski from St. Petersburg State University of Information Technologies, Mechanics and Optics (Russia) for useful discussions of the results presented in this paper.

APPENDIX: GUIDED MODES IN THE SLAB OF WIRE MEDIUM

A closely spaced chain of half-wavelength wires [16] (one-dimensional Yagi antenna array) can be regarded as a waveguide formed by resonant scatterers. This structure is in a certain sense the microwave analog of optical plasmonic waveguides [17–19]. A slab of wire medium can be considered as a two-dimensional analog of the one-dimensional Yagi antenna array. The eigenmodes of such a waveguide were studied in [20], but the wire medium was modeled as a local dielectric. Below, we derive the dispersion equation for the eigenmodes taking into account both the spatial dispersion effects [6], and the additional boundary condition proposed in [8].

Let us consider a slab of wire medium with thickness d (see Fig. 2), and investigate if this structure can support guided modes traveling along the y direction with some propagation constant q. A guided mode must have TM polarization with respect to the wires, since the wire medium is transparent to the other polarization. Then, the total magnetic field (directed along the z axis) can be written as in (6), but without the term corresponding to the incident wave since the guided mode is only supported by its own field. The application of the boundary conditions formulated in [8] (the continuity of all components of both magnetic and electric fields at the interface between free space and the wire medium and, consequently, the continuity of the magnetic field and of its both first and second derivatives by x) at both interfaces $x=0$ and $x=d$ provides a homogeneous system of equations similar to (7) (the system is homogeneous due to the absence of the incident wave). A nontrivial solution of the system exists only if the determinant of the matrix in (7) vanishes. This yields the following dispersion equation:

$$\left[1+\frac{\gamma_{\mathrm{TM}}k_y^2\tanh\left(\frac{\gamma_{\mathrm{TM}}d}{2}\right)-kk_p^2\tan\left(\frac{kd}{2}\right)}{\gamma_x(k_y^2+k_p^2)}\right] \times\left[1+\frac{\gamma_{\mathrm{TM}}k_y^2\mathrm{ctanh}\left(\frac{\gamma_{\mathrm{TM}}d}{2}\right)+kk_p^2\mathrm{ctan}\left(\frac{kd}{2}\right)}{\gamma_x(k_y^2+k_p^2)}\right]=0. \quad (A1)$$

The dispersion equation (A1) is transcendental, and so cannot be solved analytically. Its numerical solution is presented

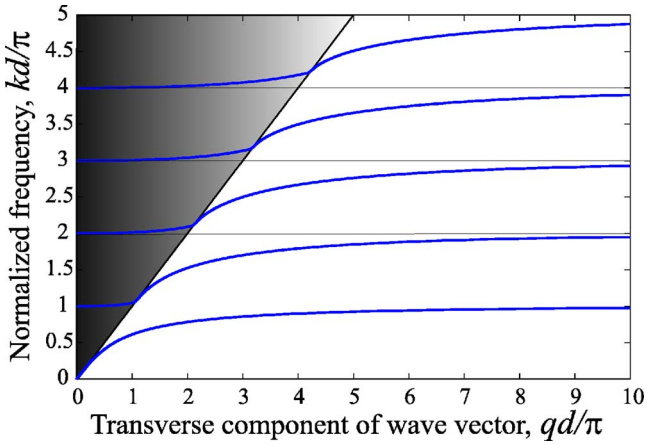

FIG. 12. (Color online) Dispersion diagram for the wire medium waveguide. The region above the light line ($q=k$) corresponding to the leaky wave region is shadowed.

in Fig. 12 in the form of a dispersion diagram. The parameters of the wire medium slab are the same as in the whole paper: $a=1$ cm, $r=1$ mm, and $d=15$ cm ($k_p d/\pi=11.3$). One can see that the slab of wire medium supports guided modes (when q is a real number and $q>k$) for nearly all frequencies, except for very narrow bands that occur near resonances that correspond to an integer number of half-wavelengths across the slab ($d=n\lambda/2$, where n is an integer). In this case the eigenmodes are leaky waves [$\mathrm{Im}(q)\neq 0$ and $\mathrm{Re}(q)<k$]. The dispersion curves for the leaky modes are presented in the shadowed region in Fig. 12. Only the real part of the propagation constant q is shown for the leaky modes.

The peaks of the transmission coefficient observed in Figs. 5 and 7 are caused by the resonant excitation of the guided modes described in this Appendix. Mathematically, this effect can be readily explained, because when the dispersion equation (A1) is fulfilled the determinant of the matrix in (7) vanishes, and consequently the reflection and transmission coefficients (8) and (9) have poles. Thus, when an evanescent plane wave with transverse component of the wave vector k_y equal to the propagation constant q of the guided mode illuminates the slab, the transmitted wave is very much amplified because of the described resonant phenomenon. Note that in Fig. 6 the resonances are absent for $1\leqslant kd/\pi\leqslant 1.06$ since the guided modes do not exist in the considered frequency range and the leaky modes cannot be excited.

[1] P. A. Belov, C. R. Simovski, and P. Ikonen, Phys. Rev. B **71**, 193105 (2005).
[2] J. B. Pendry, Phys. Rev. Lett. **85**, 3966 (2000).
[3] W. Rotman, IRE Trans. Antennas Propag. **10**, 82 (1962).
[4] J. Brown, Prog. Dielectr. **2**, 195 (1960).
[5] J. B. Pendry, A. J. Holden, W. J. Stewart, and I. Youngs, Phys. Rev. Lett. **76**, 4773 (1996).
[6] P. A. Belov, R. Marques, S. I. Maslovski, I. S. Nefedov, M. Silverinha, C. R. Simovski, and S. A. Tretyakov, Phys. Rev. B **67**, 113103 (2003).
[7] P. A. Belov, Y. Hao, and S. Sudhakaran, Phys. Rev. B **73**, 033108 (2006).
[8] M. Silveirinha, e-print: cond-mat/0509612 IEEE Trans. Antennas. Propagat. (to be published).
[9] T. Wu, *Frequency-selective Surface and Grid Array* (Wiley, New York, 1995).
[10] P. Belov, S. Tretyakov, and A. Viitanen, J. Electromagn. Waves Appl. **16**, 1153 (2002).
[11] V. Agranovich and V. Ginzburg, *Spatial Dispersion in Crystal Optics and the Theory of Excitons* (Wiley-Interscience, New York, 1966).
[12] G. Agarwal, D. Pattanayak, and E. Wolf, Phys. Rev. B **10**, 1447 (1974).
[13] J. L. Birman and J. J. Sein, Phys. Rev. B **6**, 2482 (1972).
[14] C. Luo, S. G. Johnson, J. D. Joannopoulos, and J. B. Pendry, Phys. Rev. B **68**, 045115 (2003).
[15] M. Silveirinha and C. A. Fernandes, IEEE Trans. Microwave Theory Tech. **51**, 1460 (2003).
[16] S. A. Maier, M. L. Brongersma, and H. A. Atwater, Appl. Phys. Lett. **78**, 16 (2001).
[17] S. A. Maier, P. G. Kik, and H. A. Atwater, Phys. Rev. B **67**, 205402 (2003).
[18] S. A. Maier, M. L. Brongersma, P. G. Kik, and H. A. Atwater, Phys. Rev. B **65**, 193408 (2002).
[19] W. H. Weber and G. W. Ford, Phys. Rev. B **70**, 125429 (2004).
[20] I. S. Nefedov and A. J. Viitanen, Electromagn. Waves **51**, 167185 (2005).
[21] Nevertheless one should keep in mind that the theoretical model is no longer valid when $k_y a>\pi$.